Turkish Journal of Computer and Mathematics Education Vol.12 No.8 (2021), 163-169

Research Article

Detecting macular edema through optical coherence tomography images Segmentation based on Watershed algorithm

Anjali Shelkikar[1], Vikas Humbe[2] , Ramesh Manza[3]

[1]Department of Computer Science and Information Technology, Dr. Babasaheb Ambedkar Marathwada University, Aurangabad, Maharashtra, India
[2]School of Technology, Swami Ramanand Teerth Marathwada University, Sub - Campus Latur, Maharashtra, India
[3]Department of Computer Science and Information Technology, Dr. Babasaheb Ambedkar Marathwada University, Aurangabad, Maharashtra, India

Article History: Received: 10 January 2021; Revised: 12 February 2021; Accepted: 27 March 2021; Published online: 20 April 2021

Abstract: In this paper, Optical Coherence Tomography is used to imaging DME image cells in order to assess their properties and calculate their consistency. Firstly, the median filter and morphological operations were used in the experiment. This approach improves image quality and resolves OCT image problems. For statistical analysis, the dataset is used. The DME images were automatically segmented.

Keywords: Optical Coherence Tomography, Digital Image Processing, Watershed Transformation, Automatic Segmentation.

1. Introduction

The term tomography refers to the method of producing two-dimensional data derived from three-dimensional object to construct a slice image of the solid object's internal structure [1]. In the last decade, many tomographic imaging techniques have been developed, like Ultrasound, Magnetic Resonance Imaging (MRI) and Computer-Generated Imaging [2]. Optical Coherence Tomography is a fundamentally novel technique of optical imaging modality. This technique has been developed for noninvasive cross sectional imaging in biological systems [3]. Furthermore, OCT has a determinant role in imaging due to the accuracy of micrometer resolution and millimeter penetration depth.

Optical Coherence Tomography is based on the detection of infrared light waves to acquire micron scale, cross-sectional, and three dimensional (3D) image of the subsurface microstructure of biological tissues. It is analogous to B-mode ultrasound imaging, except that the echo time delay and the intensity of back-reflected or back-scattered infrared light instead of the acoustic waves, is measured. The principal operation of OCT is based on fiber optic Michelson interferometer, which performs measurements with a low coherence length light source. The “sample arm” of the interferometer illuminates the light on the tissue and collects the backscattered light and the “reference arm” of the interferometer has a reference path delay that is scanned as a function of time. Optical interference between the light from the sample and the reference arms occurs only when the optical delays correspond to within the coherence length of the light source [1]. Two basic approaches of OCT have been developed through the years, the Time Domain OCT (TD OCT) and the Fourier or Frequency Domain OCT (FD OCT).

Optical Coherence Tomography is a novel noninvasive, high-resolution tomographic imaging technique using near-infrared light to acquire micron scale, cross-sectional, and three dimensional (3D) image of the subsurface microstructure of biological specimens in situ and in real time, which introduced in 1991. OCT imaging has a number of features that make it attractive for a wide range of application.

1. Application of Optical coherence tomography

Optical Coherence Tomography has evolved from an experimental laboratory tool to a new diagnostic imaging modality with a wide spectrum of clinical applications in medical practice including ophthalmology, cardiology, oncology, gastroenterology, dermatology, dentistry, urology, gynecology among others [1]. OCT was initially applied for imaging in ophthalmology. Nevertheless, additional advances in OCT technology have made it possible to use OCT in a wide variety of applications. Medical applications are still dominating in the OCT application. Besides the closely related surface tomography techniques, only a few non-medical OCT applications have been investigated so far [4].

a.Most developed medical OCT applications:

Ophthalmology: Ophthalmic applications of OCT have been expanded rapidly, due to the reason of the relatively transparent nature and accessibility of the human eye [1]. Another reason is the interferometric sensitivity and precision of OCT which fits quite well the near-optical quality of many ophthalmological structures. Still another reason is the independence of depth resolution from sample beam aperture which enables high sensitivity layer structure recording at the fundus of the eye [4]. It constitutes an invaluable diagnostic tool in the areas of retina diseases and glaucoma [1].

Cardiology: The domain of cardiology has been extensively investigated. Firstly, OCT was applied to the examination of coronary artery structure and the evaluation of atherosclerotic plague morphology and stenting complications. Subsequently, cellular, mechanical, and molecular analysis was performed including the estimation of macrophage load. Moreover, the application of OCT to cardiology was greatly enhanced by technological developments such as rotational catheter-based probes, very high imaging speed systems, and functional OCT modalities [1].

Oncology: Imaging has been performed in a wide range of malignancies including gastrointestinal, respiratory and reproductive tract, skin, breast, blander, brain, ear, nose, and throat cancers. OCT has been used to evaluate the larynx, and has been shown to effectively quantify the thickness of the epithelium and evaluate the integrity of the basement membrane. It was also used to visualize the structure of the lamina propria [1]. Moreover there are additional applications for oncology but is at the experimental level. This is happen because of

the improvement of accuracy needed.

b. Non-medical OCT applications:

Low-coherence interferometry has already been used in optical production technology and other technical fields. For example, LCI or 'interference with white light' has been used for many years in industrial metrology, e.g. as position sensor , for thickness measurement of thin films , and for other measures that can be converted to a displacement. Recently, LCI has been proposed as a key technology for high density data storage on multilayer optical discs [4].

2. Proposed Methodology

The image processing technology is used in our proposed algorithm.

a. Database:

Our proposed method used 30 images, 15 are normal and 15 are macular edema images.

A. input image

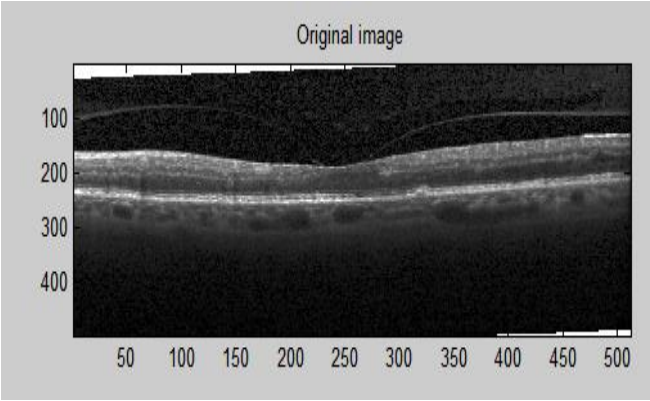

Figure 1: Original Image

Figure 2: (a) Original Image (b) Binary Image (c) distance metric, (d) watershed

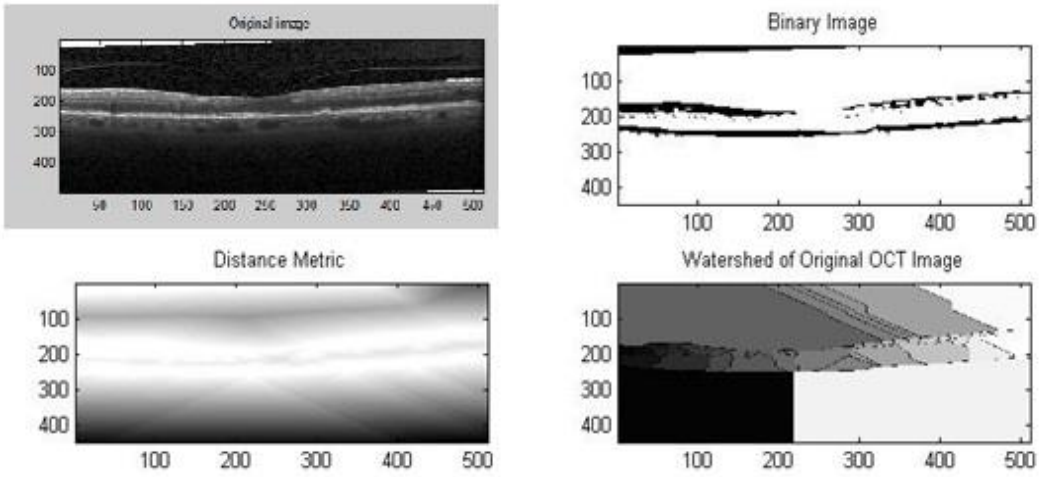

B. Conversion of the OCT Image to Binary

In this step, the threshold level computed with the usage of Otsu Algorithm, as referred before, and the intensity grayscale image converted to binary image.

C. Distance Metric

A tool commonly used in conjunction with the watershed transform for segmentation is the distance transform. The Distance Transform of a binary image is a relative simple concept: It is the distance from every pixel to the nearest non zero-valued pixel. The method which is used to compute the distance transform was the chessboard. The chessboard distance between (x1, y1) and (x2, y2) is max (|x1 - x2|,| y1 - y2|).

The above Figure 2: (c) distance metric Oct of DME image. This image has a maximum value at the center of each cell and a minimum at the periphery.

D. Image Segmentation based on Watershed Transform

To segment the image into homogeneous regions that corresponds to the cells of the OCT Image, Watershed Transform has been performed.

The Watershed Transform can be used to solve a variety of image segmentation problems. The watershed transform finds the catchment basins and ridge lines in a gray scale image. In terms of solving image segmentation problems, the key concept is to change the starting image into another image whose catchment basins are the object or regions we want to identify [2].

3. Measurement of Region Properties

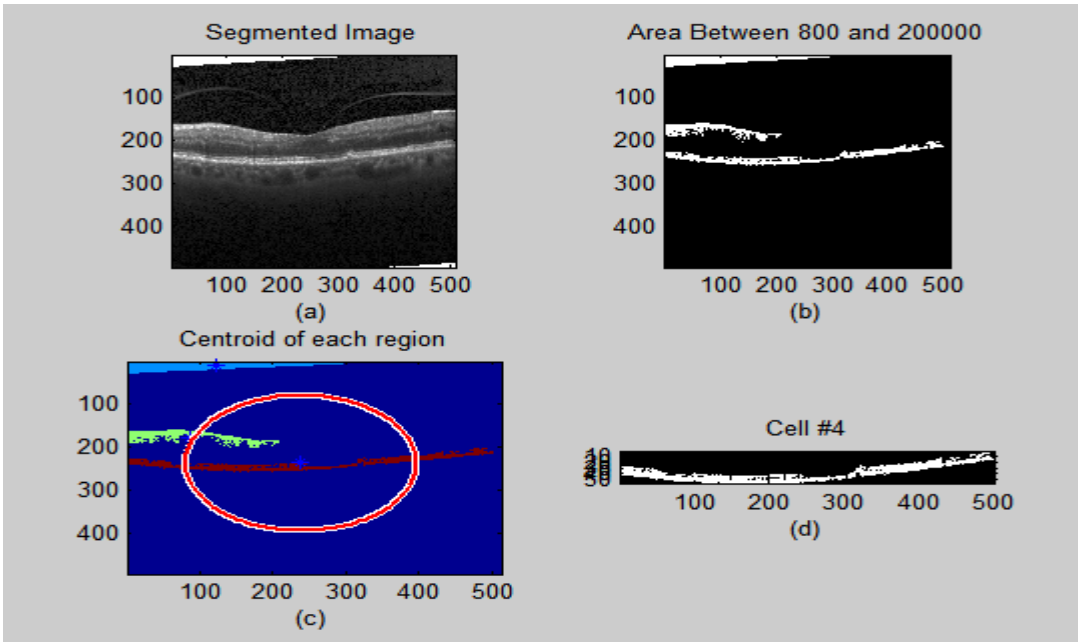

Figure 3 : (a) Binary Segment Image, (b) Binary Image containing only the region between 800 and 200,000 pixels, (c) Binary Image containing the centroid of each region (marked with *), the red circle corresponds to the cell #4, (d) Binary Image containing only the enable region (cell #4).

For the research needs, the properties that were measured are the following:

Area: the Area property returns a scalar that specifies the actual number of pixels in the region. In above Figure 3 (b), the area between 800 and 200,000 pixels is chosen in order to remove the small areas which are obtained because some outlines are not continuous.

Centroid: the Centroid property returns a 1-by-Q vector that specifies the center of mass of the region. The first element of Centroid is the horizontal coordinate (x-coordinate) of the center of mass, and the second element is the vertical coordinate (y-coordinate). Using these coordinates the centroid of each cell was plotted and the result can be found in Figure 3 (c), the centroids of each cell can be recognized by the blue star (*).

Image: the Image property returns a binary image (logical) of the same size as the bounding box of the region. The "on" pixels correspond to the region, and all other pixels are "off". In Figure 3 (d), the enable region corresponds to the cell which labeled with the number 4 Also, in Figure 3 (c) this cell represented with a red circle. In order to create this red circle the property Minor and Major Axis Length and Centroid were used to define the center and the radius of the circle.

Minor Axis Length: the minor axis length property returns a scalar that specifies the length in pixels of the minor axis of the ellipse that has the same normalized second central moments as the region.

Major Axis Length: the major axis length property returns a scalar that specifies the length in pixels of the major axis of the ellipse that has the same normalized second central moments as the region.

4. Statistical Measurement

Mean: mean and expected value are used synonymously to refer to one measure of the central tendency either of a probability distribution or of the random variable characterized by that distribution. Specifically, the sum of the observations divided by the number of the observations.

The mathematical approach for the mean can be expressed in the following formula:

$$\bar{x} = \frac{sum\ of\ observations}{number\ of\ observations} = \frac{\sum_{i=1}^{n} x_i}{n}$$

Where x' is the mean, xi is the observation, and n represents the number of observations.

Median: is the number which is separating the higher half of a data sample, a population, or a probability distribution, from the lower half. The median of a finite list of numbers can be found by arranging all the observations from lowest value to highest value and picking the middle one.

The mathematical approach for the median can be expressed in the following formula:

$$\mu = \begin{cases} x_{\left(\frac{n+1}{2}\right)}, & n\ odd \\ \dfrac{x_{\left(\frac{n}{2}\right)} + x_{\left(\frac{n+1}{2}\right)}}{2}, & n\ even \end{cases}$$

Where μ is the mean, x is the observation, and n represents the number of observations.

Variance: measures how far a set of numbers (observations) is spread out. A variance of zero indicates that all the values are identical. A small variance indicates that the data points tend to be very close to the mean and hence to each other, while a high variance indicates that the data points are very spread out around the mean and from each other.

The mathematical approach for the variance can be expressed in the following formula:

$$\sigma^2 = \frac{\sum_{i=1}^{n}(x_i - \bar{x})^2}{n-1}$$

Where σ2 is the variance, xi is the observation, x' is the mean value and n represents the number of observations.

Standard Deviation: is a measure that is used to quantify the amount of variation or dispersion of set of data values. A standard deviation close to zero indicates that the data point tend to be very close to the mean of the set, while a high standard deviation indicates that the data points are spread out over a wider range of values. Standard Deviation is equal to the positive square root of variance.

The mathematical approach for the standard deviation can be expressed in the following formula:

$$\sigma = +\sqrt{\sigma^2}$$

Name of image	Mean	Standard deviation	variance
Normal_01	0.043	0.152	0.031
Normal_02	0.031	0.134	0.027
Normal_03	0.024	0.143	0.036
Normal_04	0.037	0.164	0.026
Normal_05	0.051	0.168	0.028
Normal_06	0.011	0.184	0.024
Normal_07	0.321	0.157	0.029
Normal_08	0.652	0.174	0.021
Normal_09	0.025	0.159	0.019
Normal_10	0.012	0.169	0.027
Normal_11	0.032	0.183	0.021
Normal_12	0.045	0.162	0.026
Normal_13	0.024	0.144	0.023
Normal_14	0.033	0.198	0.022
Normal_15	0.054	0.171	0.033

Where σ is the standard deviation and the sub root (σ 2) contains the square of variance.

Table1. Statistical Measurement for Normal Images using watershed algorithm

Table2. Statistical Measurement for DME Images using watershed algorithm

Name of image	Mean	Standard deviation	variance
DME _01	0.033	0.179	0.036
DME _02	0.021	0.186	0.044
DME _03	0.034	0.184	0.039
DME _04	0.017	0.168	0.065
DME _05	0.031	0.187	0.087
DME _06	0.041	0.192	0.055
DME _07	0.032	0.177	0.022
DME _08	0.035	0.194	0.012
DME _09	0.024	0.164	0.044
DME _10	0.038	0.187	0.064
DME _11	0.039	0.191	0.041

DME _12	0.044	0.197	0.033
DME _13	0.037	0.183	0.014
DME _14	0.036	0.197	0.074
DME _15	0.023	0.174	0.014

Table 3. Average value of DME Images and Normal images

Name of feature	Normal images	DME images
Mean	0.093	0.032
Standard deviation	0.164	0.184
variance	0.026	0.042

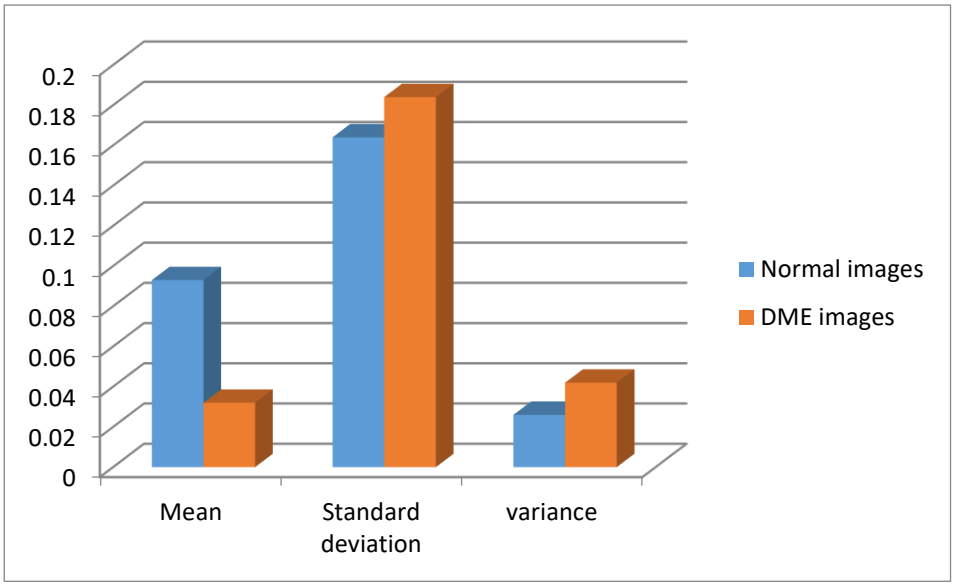

Graph1. Average value of DME Images and Normal images

5. Automatic Segmentation

Automatic segmentation is adequate to distinguish the DME images cells. The automatic segmentation is functional, accurate and reliable. Following figure4 shows (a) watershed segmented image, (b) watershed of Automatic segmented image.

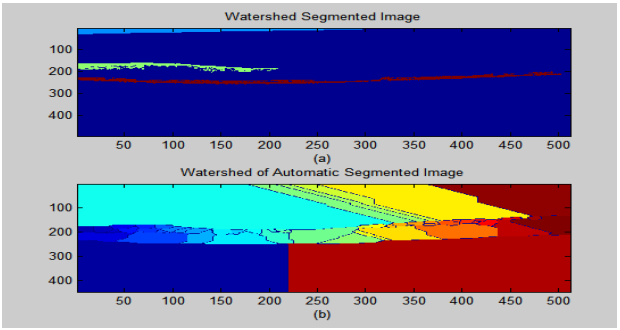

Figure 4. (a) watershed segmented image, (b) watershed of Automatic segmented image

6. Conclusion

For the purposes of this paper, the use of Optical Coherence Tomography in accordance with evolved algorithms aimed to improve the accuracy and resolution of OCT imaging. If the study produced the intended and desirable results, it would be a groundbreaking method for the researcher and a step toward improving the OCT image.

7. References

1. Chen Yu, Bousie Evgenia, Pitris Constantinos, Fujimoto G. James. Optical Coherence Tomography: Introduction and Theory
2. Gonzalez C. Rafael, Woods E. Richard, Eddins L. Steven. "Digital Image Processing Using Matlab"
3. Huang David, Swanson A. Eric, Lin P. Charles, Schuman S. Joel, Stinson G. William, Ghang Warren, Hee R. Michael, Flotte Thomas, Gregory Kenton, Puliafito A. Carmen, Fujimoto G. James. "Optical Coherence Tomography". Science. Volume 254.
4. A F Fercher, W Drexler, C K Hitzenberger, T Lasser. "Optical Coherence Tomography – Principles and Applications", January 2003.
5. Fiakkou, M. (2015). Optical Coherence Tomography Imaging For The Evaluation Of Watermelon Properties (Doctoral Dissertation, University Of Cyprus).
6. Rafael C.. Gonzalez, Richard E.. Woods, & Steven L.. Eddins. (2010). Digital image processing using Matlab®. McGraw Hill Education.
7. Huang, D., Swanson, E. A., Lin, C. P., Schuman, J. S., Stinson, W. G., Chang, W. & Puliafito, C. A. (1991). Optical coherence tomography. Science, 254(5035), 1178-1181.
8. Walther Julia, Caertner, Cimalla Peter, Burkhardt Anke, Kirsten Lars, Meissner Sven, Koch Edmund.(2011). Optical Coherence Tomography in biomedical research. Volume 400. pp. 2721-2743.
9. Král, P., & Vrba, A. (2017). Enhanced Local Binary Patterns for Automatic Face Recognition. arXiv preprint arXiv:1702.03349.
10. Rassem, T. H., & Khoo, B. E. (2014). Completed local ternary pattern for rotation invariant texture classification. The Scientific World Journal, 2014.